

Chapter 3

Dynamic-angle spinning DAS

In the previous chapter, the orientational dependences of the chemical shift interaction and the second-order quadrupolar interaction were derived. It was shown that there exists no single spinning angle which averages the second-order quadrupolar interaction completely. Dynamic-angle spinning (DAS) was developed simultaneously by both Pines *et al.*⁴² and Virlet *et al.*⁴³ This technique is useful for obtaining high resolution isotropic spectra of quadrupolar nuclei in powdered samples. Specifically, DAS does average *both* the first-order chemical shift anisotropy and the second-order quadrupolar interaction. Previously, this technique has been used to study ¹¹B⁴⁴, ¹⁷O⁴⁵⁻⁴⁸, ²³Na^{42,49,50}, ²⁷Al⁵¹ and ⁸⁷Rb^{49,52-54} in a variety of compounds. In most of these cases, the technique of DAS provides orders of magnitude improvement in overall resolution in the isotropic dimension over MAS or static experiments. In the next section, I will review some of the theory and history of the DAS experiment.

History of DAS

The roots of dynamic-angle spinning lie in the frequency formula for a second order quadrupolar interaction. It can be seen (after recombining terms in equation 2.86) that there are three terms for a crystallite of an arbitrary orientation spinning rapidly about an axis oriented at θ with respect to the magnetic field.

$$\begin{aligned} \omega^{(2Q)}(\alpha^Q, \beta^Q, \theta) &= \omega_{iso}^{(2Q)} + A_2(\alpha^Q, \beta^Q)P_2[\cos\theta] + A_4(\alpha^Q, \beta^Q)P_4[\cos\theta] \\ \omega_{iso}^{(2Q)} &= \frac{-3(I(I+1)-\frac{3}{4})}{40\omega_I I^2 (2I-1)^2} C_Q^2 \left(1 + \frac{\eta_Q^2}{3} \right) \end{aligned} \quad (3.1)$$

The first term represents the second-order quadrupolar isotropic shift. The other two, A_2 and A_4 , represent the orientationally dependent coefficients of the second and fourth-order Legendre polynomials. Figure 3.1 shows both the second and fourth-order Legendre

polynomials. It is immediately apparent that the fourth order roots (30.56° and 70.12°) do not correspond to the second order root (54.74°). This demonstrates the *futility* of spinning about a single axis to achieve high resolution quadrupolar spectra.

The solution is to use two different spinning angles in the averaging of the quadrupolar interaction. Dynamic-angle spinning is just one of these solutions.

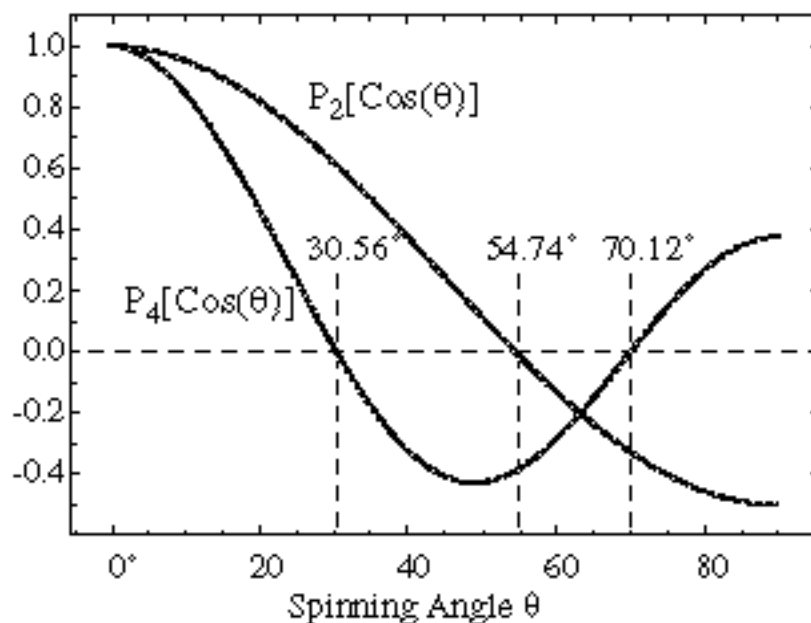


Figure 3.1 2nd and 4th Order Legendre Polynomials. There is no single angle at which both the 2nd and 4th order polynomials are zero. Therefore, multiple angles will be needed to average the second-order quadrupolar interaction (equation. 3.1).

Alternative solutions such as dynamic-angle hopping and double rotation will be discussed in chapter 6 of this thesis.^{55,56} In this experiment, the sample is allowed to undergo free precession following a 90° pulse at a first angle θ_1 for a time $t_1/(k+1)$. A z-filter is used to store the magnetization during a hopping period, in which the rotor spinning axis is changed from θ_1 to θ_2 . At a time $k t_1/(k+1)$ following the second pulse of the z-filter, a dynamic-angle spinning echo will appear. This is shown below schematically in figure 3.2. The evolution of the density matrix will be the product of two unitary

operators given by the evolution at each angle. The unitary evolution operators are shown below in equation 3.2.

$$\begin{aligned}
 U(\theta_1) &= \exp\left[-i\omega^{(2Q)}(\alpha^Q, \beta^Q, \theta_1)t_1 I_z / (k+1)\right] \\
 U(\theta_2) &= \exp\left(-i\omega^{(2Q)}(\alpha^Q, \beta^Q, \theta_2)kt_1 I_z / (k+1)\right) + \\
 &\quad \exp\left(-i\omega^{(2Q)}(\alpha^Q, \beta^Q, \theta_2)t_2 I_z\right) \\
 \rho(t_1, t_2) &= U(\theta_2)U(\theta_1)\rho(0)U^\dagger(\theta_1)U^\dagger(\theta_2)
 \end{aligned}
 \tag{3.2}$$

The assumption made in equation 3.2 is that the z-filter does not change the density matrix at all. In any single scan, this of course is impossible, however by proper choice of the phase cycle, the density matrix can be reconstructed over multiple scans so that this equation is true. The coherence pathway needed to accomplish this is shown in

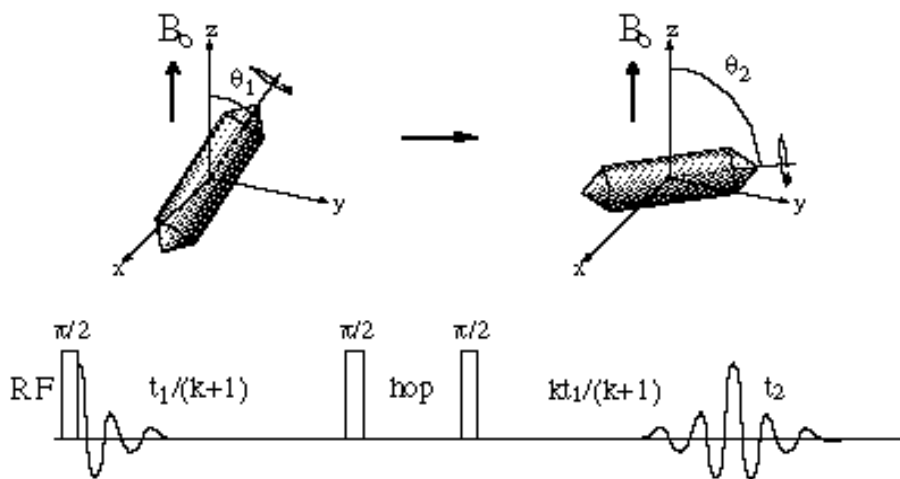


Figure 3.2 DAS Experiment and Pulse Sequence. In this experiment, the value of t_1 is incremented in a two dimensional fashion. The t_1 dimension signal gives the isotropic DAS spectrum while the second dimension contains information about the anisotropy of both the chemical shift and quadrupolar interactions.

figure 3.3. Note that the coherence is -1 both before and after the z-filter, indicating that the density matrix is unaffected by the z-filter (except for relaxation which merely scales the size of the density matrix uniformly). The minimum phase cycle needed to select this coherence pathway (assuming good receiver quadrature) is given below.

$$\begin{aligned}
& (0, 0, 0, 0), (90, 0, 0, 90), \\
(\phi_1, \phi_2, \phi_3, \phi_r) & (180, 0, 0, 180), (270, 0, 0, 270), \\
& (180, 180, 0, 0), (270, 180, 0, 90), \\
& (0, 180, 0, 180), (90, 180, 0, 270)
\end{aligned} \tag{3.3}$$

This cycle is arrived at by noticing first that we need to guarantee a -1 coherence after the first pulse and therefore cycle this pulse through 4 independent phases. The second pulse is cycled through 2 independent phases, giving either a Δp of $+1$ or -1 . Only the $+1$

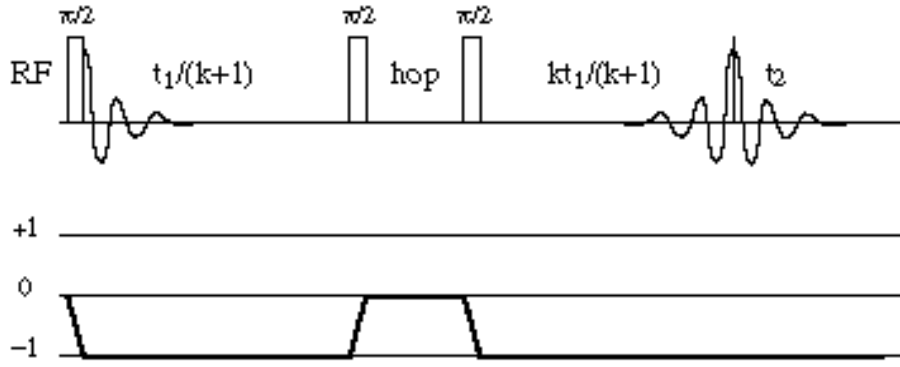


Figure 3.3 DAS Pulse Sequence Coherence Pathway. The initial -1 pathway may be selected by phase cycling the first pulse through 4 independent phases. The $+1$ Δp at the second pulse may be achieved by cycling through 2 independent phases (since the -1 Δp would produce a net -2 coherence, which cannot be present in this system). This indicates that a complete phase cycle of 8 is needed to get artifact free spectra (since the quadrature of the receiver selects the final -1 Δp).

coherence transfer is meaningful and puts the coherence at 0, which is equivalent to Zeeman order. This coherence will relax with rate T_1 during the rotor axis reorientation period, after which an uncycled 90° pulse is used to bring the coherence to the -1 level again (the $+1$ and 0 coherences will be unobservable with our receiver). The equation which describes the relationship between the phases is given below.

$$-\phi_1 + \phi_2 - \phi_3 + \phi_r = 0 \tag{3.4}$$

The observed signal may then be calculated, knowing that the initial density matrix is $\rho(0) = I_{-1}$ following the first 90° pulse.

$$\begin{aligned}
S(t_1, t_2) &= \text{tr}\{\rho(t_1, t_2)I_{+1}\} \\
&= \exp -i \frac{\omega^{(2Q)}(\alpha^\varrho, \beta^\varrho, \theta_1)t_1 + k\omega^{(2Q)}(\alpha^\varrho, \beta^\varrho, \theta_2)t_1}{(k+1)} \times \\
&\quad \exp\left[-i\omega^{(2Q)}(\alpha^\varrho, \beta^\varrho, \theta_2)t_2\right]
\end{aligned} \tag{3.5}$$

The key to the entire DAS experiment may be seen clearly in equation 3.5. If the t_1 -dependent part can be made to be purely isotropic through proper choice of θ_1 and θ_2 , then the entire problem is solved. To do this we set the t_1 -dependent sum of two terms in this exponential equal to $(k+1)\omega_{iso}^{(2Q)}t_1$ for all values of both orientation and time.

$$\begin{aligned}
(k+1)\omega_{iso}^{(2Q)}t_1 &= \omega^{(2Q)}(\alpha^\varrho, \beta^\varrho, \theta_1)t_1 + k\omega^{(2Q)}(\alpha^\varrho, \beta^\varrho, \theta_2)t_1 \\
0 &= A_2(\alpha^\varrho, \beta^\varrho)P_2(\cos\theta) + A_4(\alpha^\varrho, \beta^\varrho)P_4(\cos\theta) + \\
&\quad A_2(\alpha^\varrho, \beta^\varrho)kP_2(\cos\theta) + A_4(\alpha^\varrho, \beta^\varrho)kP_4(\cos\theta)
\end{aligned} \tag{3.6}$$

In this final expression, we know that the Legendre polynomials will not both simultaneously be zero (from figure 3.1). Also, the orientationally dependent coefficients will likewise be non-zero for most orientations. The only absolute solution is for the following pair of equations to be true.

$$\begin{aligned}
P_2(\cos\theta_1) &= -kP_2(\cos\theta_2) \\
P_4(\cos\theta_1) &= -kP_4(\cos\theta_2)
\end{aligned} \tag{3.7}$$

This guarantees that for all orientations, the anisotropic terms will cancel in the t_1 evolution, leaving a purely isotropic evolution.

$$S(t_1, t_2) = \exp\left[-i\omega_{iso}^{(2Q)}t_1\right] \exp\left[-i\omega^{(2Q)}(\alpha^\varrho, \beta^\varrho, \theta_2)t_2\right] \tag{3.8}$$

Equation 3.7 is a system of two equations with three unknowns. This means that there will be a continuous distribution of solutions which may be parameterized by k . These angles are shown below in figure 3.4. The usual pair of angles used for DAS experiments are the $k = 1$ pair (37.38° and 79.19°) and the $k = 5$ pair (0.00° and 63.43°). The reasons

for the choice of $k = 5$ or $k = 1$ will be discussed later, however, any other angle pair meeting the criterion of equation 3.7 will work as well. The solutions (as a function of k)

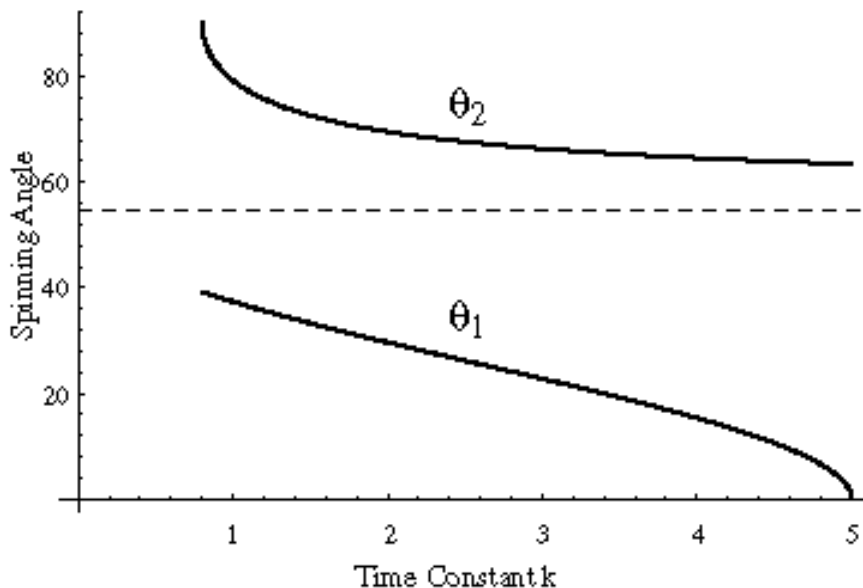


Figure 3.4 DAS Angle Pairs. The angles θ_1 and θ_2 are solutions to equation 3.6 as parameterized by k given in equation 3.9. It is interesting to note that the magic-angle (shown with a dotted line) is not included in the possible solutions to the DAS equations.

to the pair of equations 3.7 are given below and were used to generate the curves in figure 3.4.

$$\cos \theta_1 = \sqrt{\frac{1 + 2\sqrt{\frac{k}{5}}}{3}} \quad (3.9)$$

$$\cos \theta_2 = \sqrt{\frac{1 - 2\sqrt{\frac{1}{5k}}}{3}}$$

One of the first *samples* for which a DAS spectrum was collected was from the ^{23}Na nucleus in sodium oxalate ($\text{Na}_2\text{C}_2\text{O}_4$).⁴² The spectrum in figure 3.5 represents the Fourier transform of the DAS echo tops which corresponds to the signal at $t_2 = 0$. This spectrum was taken at a magnetic field strength of 11.7T (132.7 MHz for ^{23}Na) with a homebuilt DAS probe which has been designed by Mueller *et al.*^{15,51} The angle pair for this experiment is the $k = 1$ set of 37.38° and 79.19° . This represents a total of 512 scans

for each of the 128 t_1 points which have been zero filled to 512 points before Fourier transforming. The ^{23}Na $\pi/2$ central transition selective pulses were $5.0 \mu\text{s}$ while the

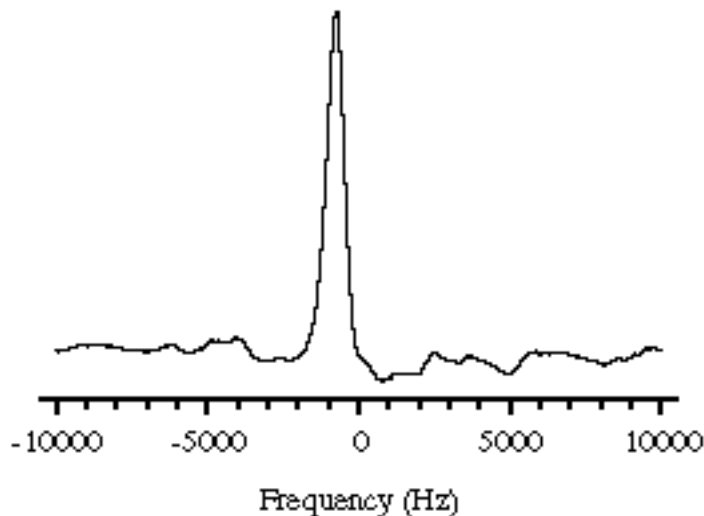


Figure 3.5 Example 1D DAS Spectrum of Sodium Oxalate. This spectrum was acquired at 11.7T by Fourier transforming the DAS echo tops taken at $t_2 = 0$.

hopping time was 30.0 ms. The magic-angle was set using the usual method of maximizing the number of ^{81}Br spinning sidebands present in an internal KBr angle standard (^2H in deuterated HMB or DMB will also work equally well) as has been discussed previously.¹⁵ The overall linewidth of the isotropic site is about 700 Hz. This is significantly narrower than the approximately 3-4 kHz wide line seen in variable-angle spectra of sodium oxalate. The theory for the limiting linewidth of DAS peaks such as this will be described in the last section of this chapter.

Dynamic-angle spinning data may alternatively be processed by Fourier transforming with respect to both dimensions. The resulting two-dimensional DAS spectrum has phase twist lineshape (see chapter 4) and to make the data presentable, it is viewed in magnitude mode (where this operation is performed by calculating the magnitude of each complex point in the spectrum). The 2D DAS spectrum is shown for sodium oxalate in figure 3.6. This experiment has 128 points in t_1 (the isotropic DAS dimension) and 128 points in t_2 (the anisotropic VAS dimension). Other parameters are identical to the previ-

ous spectrum. The spectral width in each dimension is indicated on the plot. The projections onto both axes are shown on top and to the right of the contour plot. Notice that

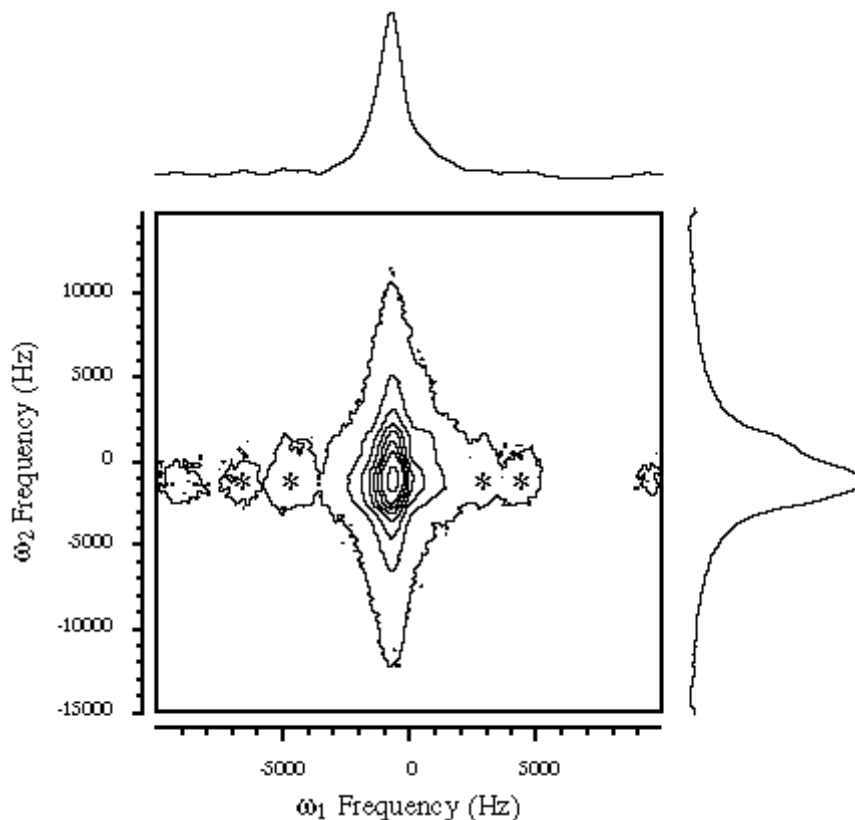


Figure 3.6 Example 2D DAS Spectrum of Sodium Oxalate. This spectrum was acquired at 11.7T by performing a 2D Fourier transform of the DAS data set. The data is presented in magnitude mode to avoid the phase twist lineshapes. Asterisks indicate spinning sidebands.

two spinning sidebands on either side of the isotropic peak are indicated with asterisks. The theory describing both their intensity and position will be presented in the next section. Also, it is apparent that the presentation of the data in magnitude mode leads to much broader lines than the absorption mode 1D spectrum seen in figure 3.5 (compare to the isotropic projection onto the ω_1 dimension in figure 3.6). A method for acquiring pure-absorption phase spectra in two dimensions will be discussed in chapter 4. These spectra demonstrate the potential of DAS to successfully average second-order quadrupolar interactions.